3-D MAGNETIC FIELD CONFIGURATION LATE IN A LARGE TWO-RIBBON FLARE

R. L. MOORE
Space Sciences Laboratory, ES82, NASA/Marshall Space Flight Center, Huntsville, AL 35812, U.S.A.

B. SCHMIEDER
Observatoire de Paris, Section de Meudon, DASOP, F-92195 Meudon, France

D. H. HATHAWAY
Space Sciences Laboratory, ES82, NASA/Marshall Space Flight Center, Huntsville, AL 35812, U.S.A.

T. D. TARBELL
Lockheed Palo Alto Research Laboratories, 91-30 252, 3251 Hanover Street, Palo Alto, CA 94304-1121, U.S.A.

(Received 14 February 1997; accepted 25 March 1997)

Abstract. We present Hα and coronal X-ray images of the large two-ribbon flare of 25–26 June, 1992 during its long-lasting gradual decay phase. From these observations we deduce that the 3-D magnetic field configuration late in this flare was similar to that at and before the onset of such large eruptive bipolar flares: the sheared core field running under and out of the flare arcade was S-shaped, and at least one elbow of the S looped into the low corona. From previous observations of filament-eruption flares, we infer that such core-field coronal elbows, though rarely observed, are probably a common feature of the 3-D magnetic field configuration late in large two-ribbon flares. The rare circumstance that apparently resulted in a coronal elbow of the core field being visible in Hα in our flare was the occurrence of a series of subflares low in the core field under the late-phase arcade of the large flare; these subflares probably produced flaring arches in the northern coronal elbow, thereby rendering this elbow visible in Hα. The observed late-phase 3-D field configuration presented here, together with the recent sheared-core bipolar magnetic field model of Antiochos, Dahlburg, and Klimchuk (1994) and recent *Yohkoh* SXT observations of the coronal magnetic field configuration at and before the onset of large eruptive bipolar flares, supports the seminal 3-D model for eruptive two-ribbon flares proposed by Hirayama (1974), with three modifications: (1) the preflare magnetic field is closed over the filament-holding core field; (2) the preflare core field has the shape of an S (or backward S) with coronal elbows; (3) a lower part of the core field does not erupt and open, but remains closed throughout flare, and can have prominent coronal elbows. In this picture, the rest of the core field, the upper part, does erupt and open along with the preflare arcade envelope field in which it rides; the flare arcade is formed by reconnection that begins in the middle of the core field at the start of the eruption and progresses from reconnecting closed core field early in the flare to reconnecting 'opened' envelope field late in the flare.

1. Introduction

The SCOSTEP/STEP WG-1 Workshop on Measurements and Analyses of the 3-D Solar Magnetic Fields was held in Huntsville, Alabama, 9–11 April, 1996. A highlight of the Workshop was that several recent observations and ideas about the large-scale 3-D magnetic field in and around large filaments and two-ribbon

Solar Physics **176:** 153–169, 1997.

eruptive flares were presented and avidly discussed. The present paper was sparked by those discussions.

One focus of the Workshop was the large-scale twist in solar magnetic fields: on scales of active regions and larger, many bipolar magnetic fields on the Sun have an overall twist. This has been established empirically in the past several years by studies of the structure of chromospheric filaments (Martin, Bilimoria, and Tracadas, 1994) and by detection of large-scale magnetic twist in photospheric vector magnetograms of active regions (Gary *et al.*, 1987; Pevtsov, Canfield, and Metcalf, 1995). See Schmieder *et al.* (1996a) for a clear example of a bipolar active region having chromospheric Hα fibril structure and coronal X-ray loops that show the magnetic field in the interior of the bipole to have a definite overall shear and twist. At the workshop, D. Rust presented further evidence for such large-scale magnetic twist. This new evidence is from the *Yohkoh* SXT coronal X-ray images of the onsets of large-scale, bipolar, long-duration eruptive solar flares (Rust and Kumar, 1996). At the onset of these eruptions, plasma in the core magnetic field (that is, in the field close to the polarity inversion line in the core of the flaring bipole) brightens in the SXT coronal images. The brightened feature has the overall shape of either a letter S or a backward S, the middle of which traces the polarity inversion line. These observations confirm what is well established from the structure of chromospheric filaments and from vector magnetograms: the core field of these eruptive-flare bipoles is strongly sheared, that is, the core field runs along the inversion line rather than going right over it as an unsheared (potential) field would (e.g., Moore and Roumeliotis, 1992). In addition, the observed shape shows that at and before eruption onset the core field is globally twisted. An S shape is the signature of right-handed twist; a backward-S shape signifies left-handed global twist.

Also at the Workshop, R. Moore presented other examples of large-scale bipolar eruptive flares for which the *Yohkoh* SXT coronal images showed such sheared and globally twisted field in the core of the closed bipolar field at and before the start of the eruption (Moore *et al.*, 1996); for three recently published examples, see Manoharan *et al.* (1996), Hudson, Acton, and Freeland (1996), and Pevtsov, Canfield, and Zirin (1996). In these cases, the SXT coronal images appear to confirm the preflare 3-D magnetic field configuration proposed by Moore and LaBonte (1980) from ground-based photospheric and chromospheric images and Skylab coronal X-ray images before and during a large eruptive flare. The preflare field configuration drawn by Moore and LaBonte from the observations of that flare is the one on the left in Figure 1. As the drawing shows, in this case the global twist of the core field was left-handed and the overall shape of the core field was that of a backward S. For either sense of global twist and shape of the core field, the *Yohkoh* coronal images, together with the findings of Martin, Bilimoria, and Tracadas (1994) on the magnetic structure of filament channels and filaments, indicate that the overall 3-D configuration of the entire preflare bipole has the following four characteristics depicted in Figure 1: (1) the preflare 3-D field configuration is an

arcade with globally twisted, strongly sheared core field; (2) the core of strongly sheared field is straddled by the rest of the arcade field, an envelope of field that is rooted farther from the polarity inversion line and is much less sheared than the core field (the field shear decreases with distance from the inversion line gradually enough that there is still some shear in the envelope field near the core field, but much less than the average shear in the core field); (3) the overall 3-D shape of the core field is that of a sculpted letter S (or backward S) lying on the Sun: the middle of the S dips under the envelope arcade, and the two curves of the S bulge upward out opposite ends of the arcade and return to the photosphere at the ends of the S; (4) the opposite ends of the S are rooted on opposite sides of the polarity inversion line. This empirical 3-D field configuration is essentially that computed by Antiochos, Dahlburg, and Klimchuk (1994) in their force-free model for a 3-D closed bipole with sheared core. In the opening talk of the Workshop, S. Antiochos presented this self-consistent magnetostatic field model for sheared-core bipoles and pointed out that this model gives the overall S shape of observed large-scale bipolar solar fields and explains why these fields dip in the middle of the S so that a cool filament can form and be held there over the inversion line, as in the preflare sketch in Figure 1.

The large-scale flares that erupt in these sheared-core bipolar fields are traditionally called two-ribbon flares because of their characteristic pattern of brightening in the chromosphere (Dodson-Prince and Bruzek, 1977; Švestka and Cliver, 1992). Soon after flare onset, the chromospheric flare takes the form of two bright ribbons that bracket the inversion line and rapidly grow wider by expanding away from the inversion line. By late in the decay phase the two ribbons become thinner, shorter, and farther apart, and their migration away from the inversion line is much slower than early in the flare. A growing arcade of X-ray flare loops and Hα post-flare loops straddles the inversion line and stands on the two flare ribbons (e.g., Moore *et al.*, 1980). The linkage and joint evolution of the flare arcade and ribbons is apparently the result of reconnection reclosing of the envelope field which was eruptively opened early in the flare. The inferred 3-D topology of the 'opened' erupted core-with-envelope field, reclosing envelope field, growing flare arcade, and separating flare ribbons in the late phase is sketched on the right in Figure 1. This basic picture for two-ribbon eruptive flares has been further supported by *Yohkoh* SXT coronal X-ray images of flares near the limb (e.g., Tsuneta *et al.*, 1992; Tsuneta, 1996; Shibata, 1996).

At the Workshop, B. Schmieder presented a study of the arcade of X-ray loops and its nested arcade of Hα post-flare loops in the decay phase of the large two-ribbon flare of 25–26 June, 1992, situated near the equator and near the west limb (N09, W70–80) (van Driel *et al.*, 1997). The flare arcade was well observed by the *Yohkoh* SXT and the Hα post-flare loop system was well observed by several ground-based observatories. Schmieder presented a spectacular pair of images of the Hα loop system (a line-center image and a Doppler velocity image) obtained with the Swedish telescope at La Palma by the Lockheed group. These images

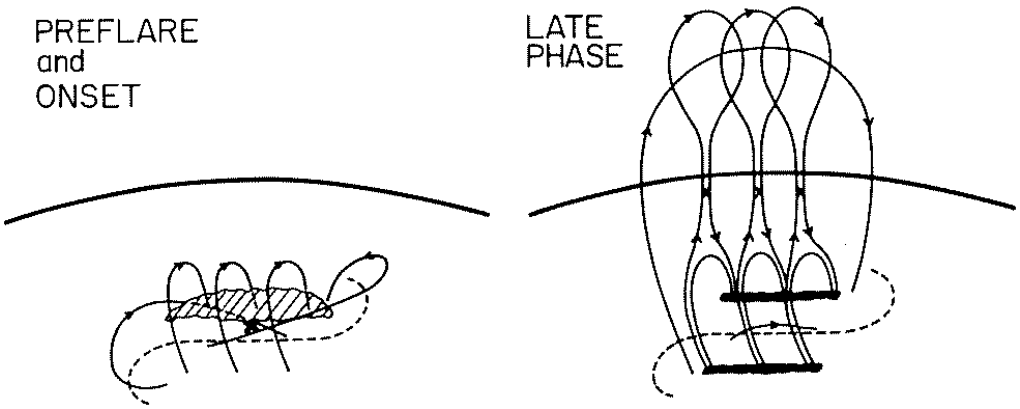

Figure 1. The 3-D magnetic field configuration and eruption model deduced by Moore and LaBonte (1980) for the large two-ribbon flare of 29 July 1973. The heavy arc is the east limb; the backward-S dashed curve is the photospheric polarity dividing line of the overall bipolar magnetic field of the flare site; curves with arrowheads are magnetic field lines; Xs mark places where reconnection occurs. The shaded feature is the large dark chromospheric filament that was suspended in the preflare backward-S sheared core field and erupted with the core field at flare onset. In this scenario, early in the eruption, reconnection occurs under the filament, between the inner legs of the core-field coronal elbows (having their outer ends in the curls of the early flare ribbons (not shown here)), releasing the upper reconnected core field to erupt upward and 'open' itself and the overarching envelope field. In the late phase, the opened envelope field recloses by reconnection, forming the growing arcade of flare loops rooted in the spreading flare ribbons. At the late stage of the flare ribbons depicted here, the 3-D topology of the magnetic field would be as shown, but the erupted field would reach far into the outer corona, much farther than in this sketch.

clearly showed the high-arching post-flare loops that were nested just inside the X-ray arcade and that had chromospheric-temperature plasma draining down their legs. These Hα images also showed that in this flare there was another system of loops that was lower and of different shape and direction than the arcade loops.

In the closing summary talk of the Workshop, D. Rabin again showed the pair of La Palma Hα images from Schmieder's presentation and suggested that the lower system of loops was additional evidence for a large-scale S-shaped 3-D field configuration of the type that had been repeatedly advocated at the Workshop. What had previously been viewed by many as a messy complication that put this flare somewhat at odds with the standard late-phase picture, Rabin saw as possible direct evidence confirming the presence of an S-shaped core field in two-ribbon eruptive flares. The purpose of this paper is to point out that the X-ray and Hα images of this flare do indeed support Rabin's insight, and that the late-phase presence of this core field structure is easily accommodated by the picture for two-ribbon eruptive flares sketched in Figure 1.

2. Observations

In this section we present five complementary images of tracers of the 3-D magnetic field in the gradual phase of the big two-ribbon flare of 25–26 June 1992. These images reinforce each other in showing that the core field straddled by the flare arcade was sheared and S-shaped.

In soft X-ray emission observed by the GOES satellite, the flare began at about 19:45 UT (25 June), grew rapidly through 20:00 UT, passed through its maximum (X 3.9) around 20:10 UT, and then entered its long-duration gradual decay phase, lasting for over 16 hours (e.g., see Schmieder *et al.*, 1996b). Through the first three hours of the decay phase the flare was observed in Hα filtergrams at Hida Observatory. One of these filtergrams is shown in Figure 2. This image, taken toward the end of the first hour of the decay phase, shows the two flare ribbons and the arcade of post-flare loops rooted in the two ribbons. The top of the arcade projects a little above the west limb. The loops of the arcade are viewed nearly end-on; that is, the loops are in mainly vertical, mainly east-west planes. The flare ribbons, and hence the magnetic polarity inversion line bracketed by the ribbons, run generally southeast-northwest. The direction of the inversion line is confirmed by the full-disk magnetograms from Kitt Peak and from Mt. Wilson on 25 and 26 June, 1992 published in *Solar-Geophysical Data*.

The image in Figure 2 displays three pieces of evidence for the presence of global shear and twist in the magnetic field and for the sense of the shear and twist. First, the two flare ribbons are seen to be offset from each other along the inversion line; the eastern ribbon clearly extends farther southeast than the western ribbon, and, even though the western ribbon is partly obscured by the post-flare loops, it is seen to extend farther northwest than the eastern ribbon. This offset in the ribbons is compatible with the direction of the post-flare loops in this image: the loops are not orthogonal to the inversion line but are somewhat sheared so that they fit the offset of the ribbons in which they are rooted; the loops appear to cross the inversion line at an angle of about 60 degrees. Second, the northwest end of the eastern ribbon bends to the west and the southeast end curls to the east, giving this ribbon the shape of an S that has a somewhat truncated top. Third, there are low-lying dark chromospheric fibrils that sweep out from the south end of the arcade and curve to the east, conforming to the curl in the eastern ribbon; these fibrils presumably trace low-lying magnetic field lines connecting opposite polarities across the inversion line. All three of these markers of magnetic structure are typically seen in Hα images of two-ribbon flares. The characteristics of the ribbons and loops seen here are typical in and before the early decay phase; chromospheric fibrils sweeping along and over the inversion line in the outskirts of the flare region are typical before, during, and after the flare (e.g., Moore and LaBonte, 1980; Moore, LaRosa, and Orwig, 1995). In Figure 2, these features indicate that the core field running under the arcade early in the decay phase had right-handed global shear and twist. The sense of the twist is indicated by the implied global S shape of the core

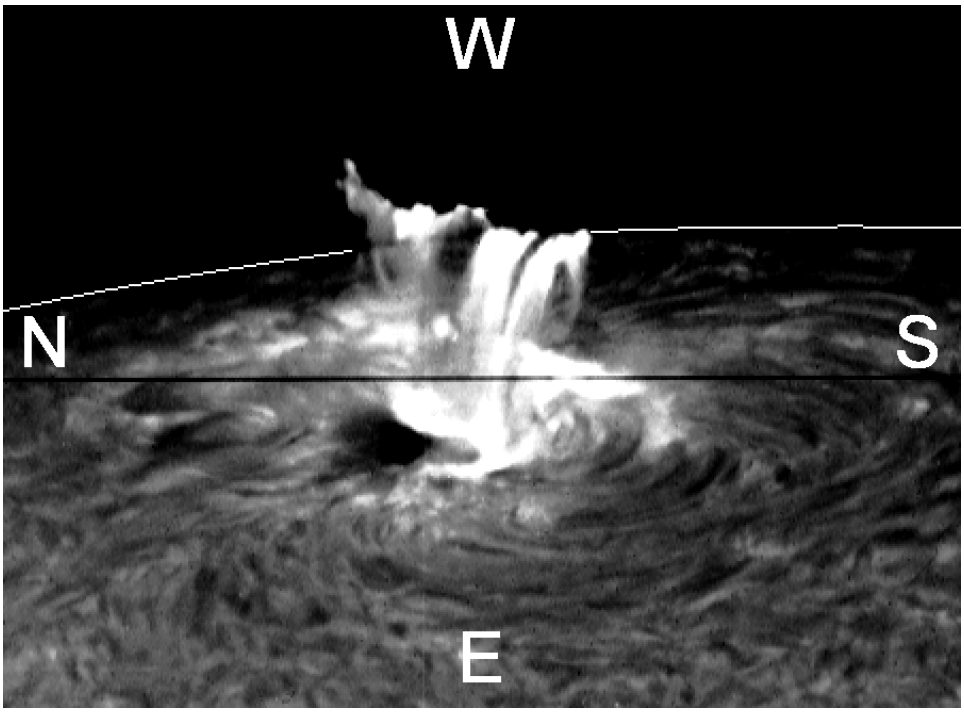

Figure 2. Flare ribbons, flare loop arcade, and chromospheric fibrils early in the decay phase of the large two-ribbon flare of 25–26 June, 1992. The background arc traces the chromospheric west limb. This Hα image (from a spectrograph slit jaw) was taken at Hida Observatory at 20:54:23 UT on 25 June, 1992.

field; the corresponding sense of shear is indicated by the sense of shear in the post-flare loops, by the sense of the offset of the two ribbons from each other along the inversion line, and by the offset of the opposite ends of the dark fibrils along the inversion line. (An offset of this sense would be given by a right-handed photospheric shear flow along the inversion line: northward flow on the west side of the inversion line and/or southward flow on the east side. This imaginary operation gives a reason for naming this sense of shear 'right-handed' (the curl vector of this horizontal shear-flow velocity field points upward), but is not necessarily the actual process that produced the observed magnetic shear. Defined in this way, the handedness of the shear in observed core fields is the same as the handedness of the of the observed twist: S-shaped core fields are observed to have right-handed twist and right-handed shear; backward-S core fields have left-handed twist and left-handed shear. Thus, the observed right-handed shear in Figure 2 implies that the core field should be S-shaped, and this is corroborated by the S shape of the eastern flare ribbon.)

Figure 3 shows an SXT X-ray image of the flare about 10 hours later than in Figure 2. The X-ray image is superposed on an SXT photospheric image showing the west limb and sunspots in the region of the flare. Due to solar rotation, the flare region is noticeably closer to the limb here than in Figure 2. The flare arcade loops seen in Figure 3 were formed much later, are much taller, and are rooted farther from the inversion line than the early post-flare loops in Figure 2 (see van Driel *et al.*, 1997). Another difference is that the loops in Figure 3 are more nearly orthogonal to the inversion line, so that the loops are seen more from the side and the arcade tunnel is seen more end-on than in Figure 2. The X-ray image in Figure 3 was taken during a C 3.4 flare that occurred low in the core field under the late-phase arcade of the X 3.9 flare. This small flare is seen in Figure 3 as a low loop with bright feet. This loop runs nearly in the same direction as the inversion line, confirming that under the arcade the core field close to the inversion line was strongly sheared. We infer that the southern foot of this flare loop is on the near side of the inversion line and the northern foot is on the far side, in order that the sense of shear of the core field be the same as that deduced from the Hα structure in Figure 2. Thus, the arcade and core X-ray loops in Figure 3 together with the Hα arcade loops and other structure in Figure 2 demonstrate that in the late phase of this large two-ribbon flare the field rooted close to the inversion line was strongly sheared and the field rooted progressively farther from the inversion line was progressively less sheared. So, it is clear from these observations that the field configuration was similar to the late-phase configuration in Figure 1 in that it was a closed bipole having a strongly sheared core within an envelope of much less shear.

In addition to the small flare seen in Figure 3, four other small (C-class) flares occurred in the core field under the arcade of the large flare during the 8 hours from 5:00 UT to 13:00 UT (Schmieder *et al.*, 1996b). That is, the 7:00 UT core-field flare of Figure 3 was part of a series of of sporadic flare heating events that happened in the core field over several hours. These heating events in the core field apparently happened independently of the high reconnection reclosing of opened envelope field that formed and heated the large flare arcade.

The late decay phase of the big flare was also followed for about an hour in high-resolution narrow-band Hα filtergrams taken with the Swedish telescope at La Palma by T. Tarbell and his team from Lockheed Palo Alto Research Laboratories (Malherbe *et al.*, 1997). These observations began about an hour after the time of the X-ray image in Figure 3 (van Driel *et al.*, 1997). These filtergrams were taken in line center and in the red and blue wings of Hα in rapid sequence. Subtraction of a red-wing image from a nearly simultaneous blue-wing image gives a Doppler velocity image. One of the line-center images, taken about an hour and a half after the X-ray image in Figure 3, is shown in Figure 4(a); the cotemporal Doppler image is shown in Figure 4(b). This is the pair of Hα images that directly precipitated this paper, the one that Schmieder showed at the Workshop and that Rabin interpreted as showing an S-shaped core field.

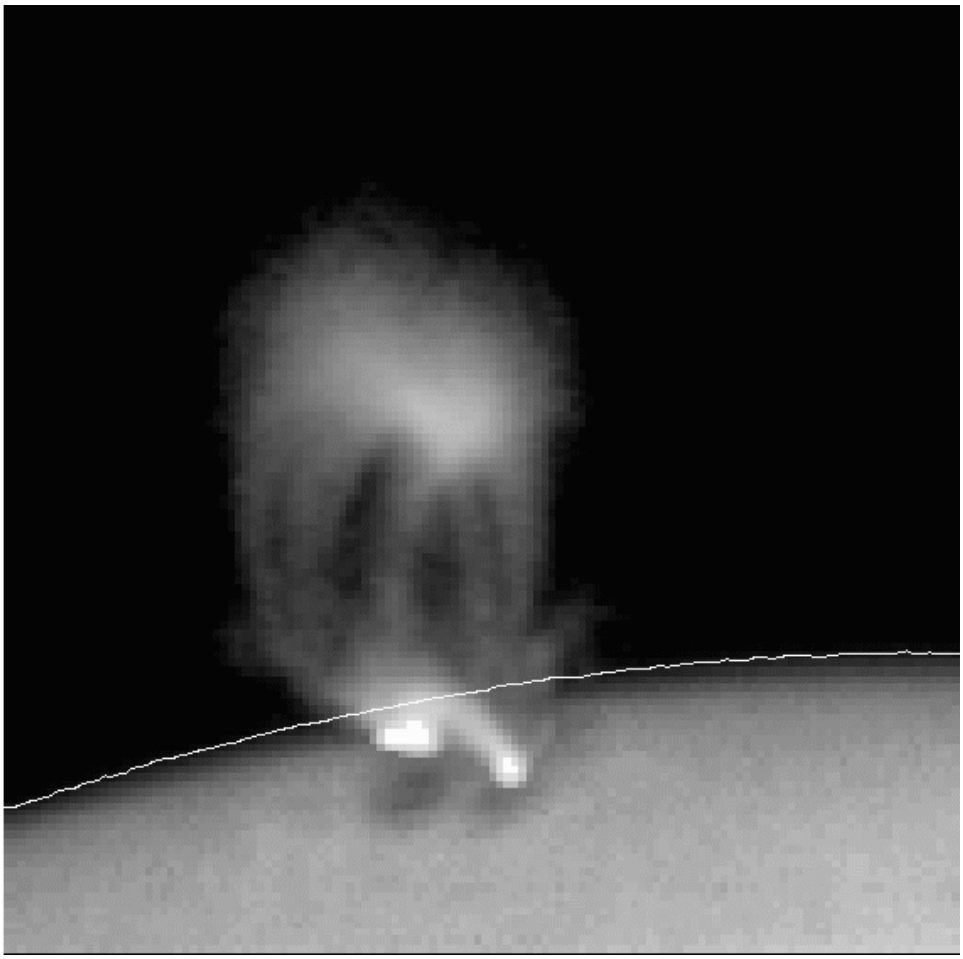

Figure 3. The large flare arcade and a subflare in the underlying core field late in the decay phase of the large flare. A *Yohkoh* SXT X-ray image of the flare (at 06:56:13 UT, 26 June) is superposed on a *Yohkoh* SXT visible-light image (taken at 07:07:25 UT) showing the sunspots in the flare region. The thin white arc traces the photospheric limb.

The post-flare arcade loops in Figure 4(a) match the X-ray flare arcade loops in Figure 3. In each of these two images, there are three prominent loops or clumps of loops in the arcade. The Hα loops are seen to have the same shape and arrangement as the X-ray loops. Van Driel (1997) (1) have shown, from superposition of Hα and X-ray images in this late phase of the flare and measurement of the heights of the loops over a time span including the times of these two images, that the Hα loops of Figure 4(a) closely trace the X-ray loops of Figure 3, and (2) have estimated the the cooling time of the X-ray loops to be $1-2$ hours. Evidently, the Hα arcade loops in Figure 4(a) are the cooled remnants of the X-ray loops in Figure 3.

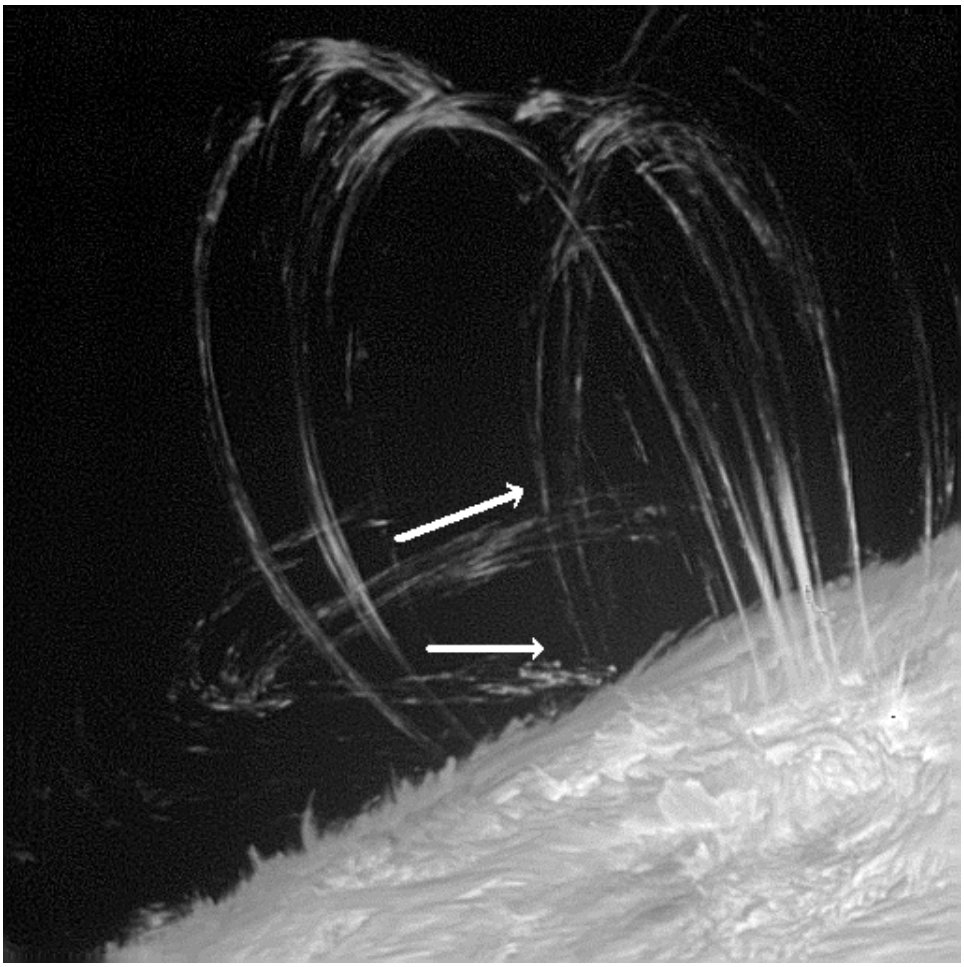

Figure 4a. The large post-flare loop system observed by the Lockheed group with the Swedish telescope at La Palma. This Hα line-center filtergram was taken at about 08:15 UT, 26 June. The arrows here and in Figure 4(b) indicate that the center-line and Doppler movies show that the Hα material all along both legs of the 'bent-over' loop was flowing downward at this time. This image has been edge-enhanced and the brightness and contrast adjusted to best show the loops above the limb. In Figures 4(b) and 4(c), the northern leg of the 'bent-over' loop is traced below the limb to its foot on the floor of the arcade tunnel.

The line-center and Doppler movies made from the sequence of Hα images show the Hα material in the arcade loops continually flowing down along the legs of the loops as usual for post-flare loops. The orientation of the arcade loops is not as obvious in the Hα image in Figure 4(a) as in the X-ray image in Figure 3. The identity of the arcade loops in these two images certifies the orientation of the Hα loops. This orientation is consistent with the blue shifts and red shifts seen in the

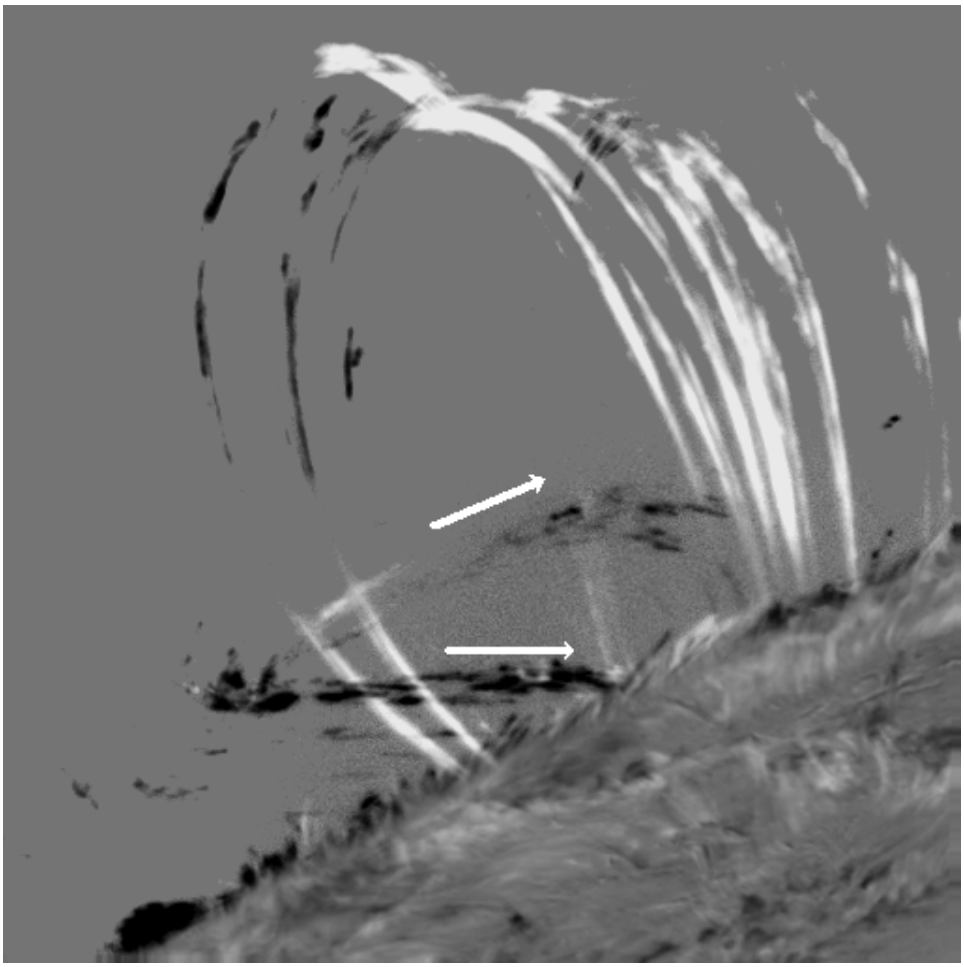

Figure 4b. The Hα Doppler image of the loop system in Figure 4(a). Material moving toward the observer is dark gray to black; material moving away is light gray to white. The northern leg of the 'bent-over' loop is strongly blue-shifted (very dark) above the limb; below the limb, this leg shows as a thin dark strand linking on down to its foot under the arcade.

Doppler image (Figure 4(b)) of the downflowing Hα material in the arcade loops. Thus, it is clear that the southern legs of all three main loops are rooted on the far side of the inversion line and the northern legs are rooted on the near side. Because the tunnel of the arcade is not orthogonal to the line of sight but is canted toward it and because the arcade is not too long, we see all the way through the projected part of the tunnel framed by the northern leg of the southern-most loop and the southern leg of the northern-most loop. For the same reason, we have a direct view of half or more of the floor of the tunnel, unobstructed by any foreground arcade loop legs. We see there (in Figure 4(c)) a thin dark filament that runs down the

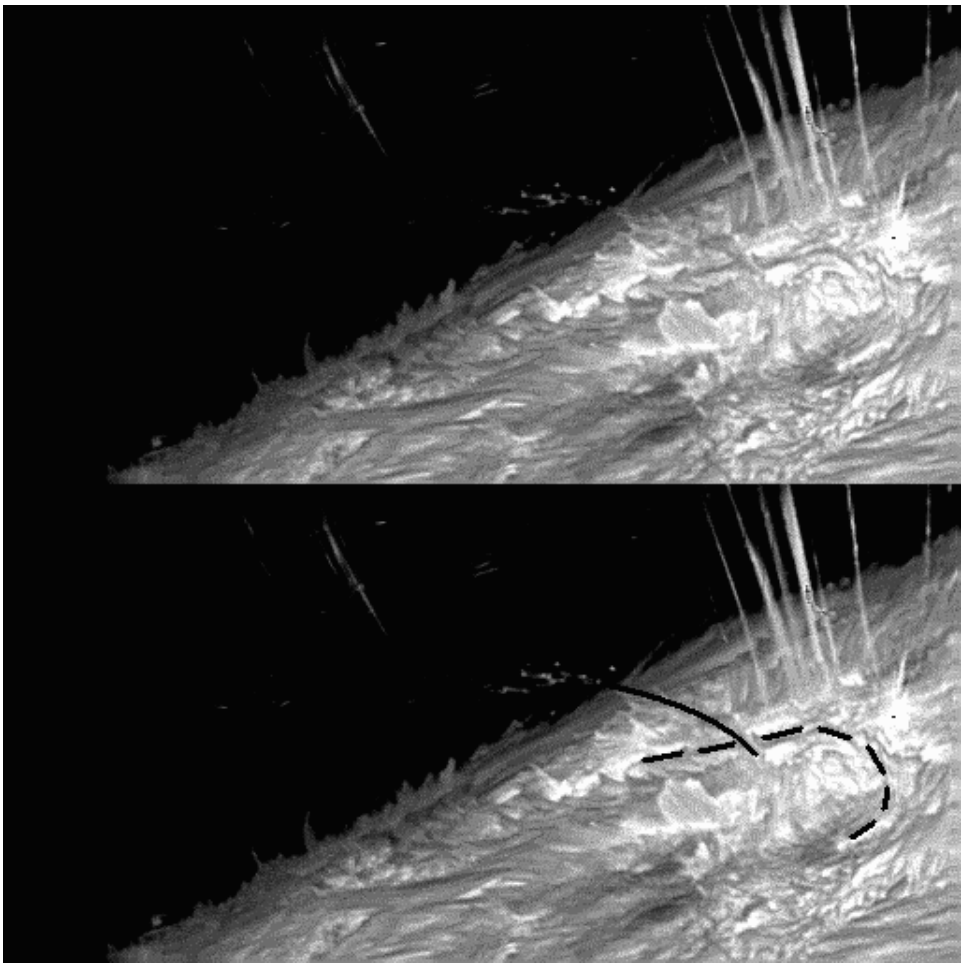

Figure 4c. Magnetic location of the foot of the northern leg of the 'bent-over' loop. The image in the top panel is the same as that in Figure 4(a) but with the brightness and contrast adjusted to best show the fibril structure under the arcade. This image is repeated in the bottom panel with two curves drawn in, tracing key structures seen in the top panel: the dashed curve is the locus of the polarity dividing line traced by the low thin filament under the arcade, and the solid curve traces the northern leg of the 'bent-over' loop below the limb. It is seen that the lower end of this leg crosses in front of the thin filament, showing that this leg of the 'bent-over' loop was rooted on the near side of the polarity dividing line.

middle of the floor of the tunnel. We take this filament to be a trace of the magnetic polarity inversion line under the arcade. This verifies the position and direction of the polarity inversion line that we adopted in discussing the orientation of the flare loops in Figures 2 and 3, and hence confirms that the flare loops in Figure 2 were moderately sheared and that the sense of the shear was right-handed.

In addition to the usual arcade of post-flare loops, Figure 4(a) shows another loop system that is seldom seen late in two-ribbon flares. These loops are lower than the arcade loops, have a strikingly different orientation than the arcade loops, and appear to be entwined in the legs of the arcade. This unusual set of loops is about the size of any of the three clumps of loops in the arcade; it looks as though it were a fourth arcade loop clump that is greatly bent over to the north so that it has an inclincation of roughly 30 deg to the horizontal. The key issue bearing on the 3-D configuration of the magnetic field is that of the 3-D trajectory of these 'horizontal' loops relative to the arcade.

The northern leg of the inclined loop clump, though much fainter below the limb than above the limb in Figure 4(a), can be followed down to its foot in the chromosphere in Figure 4(c). In Figure 4(c) (and in movies of the sequences of line-center and Doppler images as well) the foot is seen to be near the south end of the arcade tunnel and just in front of the filament marking the inversion line. This shows that the northern leg of the inclined loop system, descending from the north, enters the tunnel of the arcade and reaches almost through the tunnel. Because it runs down the tunnel and is rooted close to the inversion line, the inclined loop system is evidently part of the sheared core of the overall bipolar magnetic field of the flare region.

Because the northern leg of the inclined loops is rooted on the near side of the inversion line, we infer that the southern leg is rooted on the far side. So, we infer that at the northern extremity of these loops, where they turn sharply back to the south, they also turn to the west. That is, as they turn up and back to the south, they turn away from the viewer. This inference from the the Hα line-center image is confirmed by the Doppler image in Figure 4(b) as follows. At the time of the images in Figures 4(a) and 4(b), the line-center and Doppler movies show the Hα material throughout the inclined loops to be flowing down along the legs. (At other times, the movies show obvious upflows in these loops, often intermixed with downflows in adjacent loops or different parts of a loop.) The downflow seen at the time of Figure 4(b), together with the blue shift seen in Figure 4(b) in the sharp bend of the loops, requires that the loops bend westward in going from the northern legs to the southern legs, so that a downflow along the bend is directed partly toward the viewer. Thus, the inclined loops in Figures 4(a) and 4(b) show good evidence that they mark the core field straddled by the arcade, and that the core field is directed along the inversion line under the arcade, extends out of the north end of the arcade tunnel, bends to the west and on back around to the south-southeast, and comes down to the surface again behind the arcade. Hence, the Hα line-center and Doppler images of the inclined loops are entirely consistent with these loops tracing magnetic field lines in the northern half of an overall S-shaped sheared core field, the middle of the S tracking the inversion line under the arcade.

3. Summary of the 3-D Magnetic Field Configuration Distilled from the Observations

Figure 5 is a sketch of the observed magnetic loop structures that we have pointed out in Figures 2–4. It shows the 3-D trajectories of these loops and the way that they fit together, their mutual 3-D configuration deduced from the observations. The jagged arc represents the chromospheric limb behind the flare site. The dashed curve is the photospheric magnetic polarity dividing line straddled by this bipolar flare; the magnetic flux polarity was positive on the near side of this line and negative on the far side. The three features labeled C, B, and A are parts of the core magnetic field of the flare bipole: loop C represents the low-lying dark chromospheric filaments that sweep out from the south end of the flare arcade in Figure 2; loop B represents the core-field X-ray loop of Figure 3; loops A are the large 'bent over' loops of Figure 4. The three unlabeled large loops represent the three clumps of arcade loops in Figures 3 and 4. The observations give direct evidence for this much of the 3-D magnetic field configuration late in this large flare. Even though other parts of the 3-D field were not observed, it is clear from the observed parts sketched in Figure 5 that an S-shaped core field with right-handed twist and strong right-handed shear snaked through the tunnel of the flare arcade.

4. Discussion

The large two-ribbon flare presented in this paper was typical of this class of flares in that its flare ribbons and arcade of flare loops were of the usual form and evolved in the usual way. It was also typical in that the low-lying strands of the core field, those not reaching much above the chromosphere (such as loops B and C in Figure 5), remained greatly sheared throughout the flare. These characteristic large-scale magnetic features suggest that the global 3-D field configuration late in this flare was not exceptional for large two-ribbon flares, and hence that the core field late in these flares often has extended 'elbows' that loop to coronal heights like the one seen in this flare (loops A in Figure 5). That is, while it could be that the core field is seldom seen to have coronal elbows in the late phase of these flares because the elbows are seldom present, it seems more likely that the elbows are usually present but not seen because the conditions that reveal them are rare.

In addition to being exceptional in showing a core-field coronal elbow in Hα late in its decay phase, our flare was also exceptional in that several subflares occurred low in the core field under the flare arcade. The Hα elbow was observed during the epoch of this subflaring activity and had one leg rooted close to the site of microflaring under the arcade (in Figure 5, the foot of Hα elbow A is close to sublare X-ray loop B). This is the appropriate arrangement if the Hα elbow loop system is an example of the flaring arch phenomenon studied by Martin and Švestka (1988), Švestka *et al.* (1989), and Fontenla *et al.* (1991). A flaring arch is

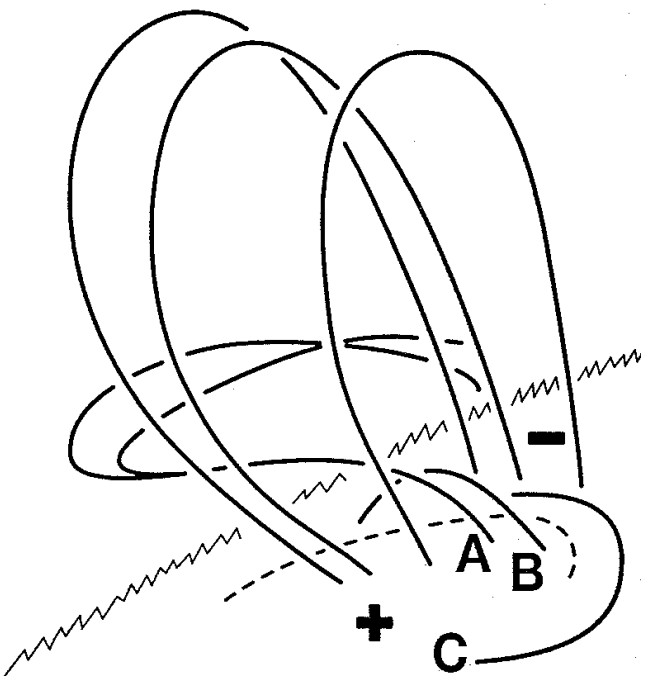

Figure 5. Summary sketch of the 3-D configuration of the main magnetic structures observed in the late phase of our large two-ribbon flare, showing that the core field extending out of the north end of the arcade had a coronal elbow with its far end rooted behind the arcade. We have deduced this 3-D magnetic field configuration directly from the observations presented in this paper. See Section 3 for detailed identification of the sketched features with observed features.

a cluster of magnetic loops that have active-region lengths, reach coronal heights, and have one end rooted at the site of a compact flare. The flare injects energetic particles and plasma into the magnetic arch. The injected plasma usually spans a wide range of temperatures, from chromospheric to coronal and hotter. In Hα movies, a flaring arch appears similar to a surge, filling by upflow from the flare foot and emptying by downflow after the flare. In the Hα movie from LaPalma, our elbow loops diplayed surging flows of this type. This behavior and the subflaring at the foot of the elbow both support the view that our flare was unusual only in displaying its core-field elbow, not in possessing a core field of this configuration late in the flare.

As was described in the Introduction, *Yohkoh* SXT coronal images have shown that for large two-ribbon flares the preflare 3-D magnetic field is a closed bipole having a sheared core field that is twisted in the shape of an S or backward S, the elbows of which bulge up into the low corona as in Figures 1 and 5. During the onset and rapid growth of the flare brightening in the chromosphere and corona, chromospheric and coronal movies have indicated that much of the core field and

its envelope field erupt and open in the manner indicated in Figure 1. At first glance, Figure 1 gives the impression that in the field eruption all of the preflare core field loses its elbows by unbending and opening along with the envelope field, and hence that in the late phase of the flare there are no coronal elbows left in the core field. However, this impression is probably wrong for many large two-ribbon flares, including the one from which Moore and LaBonte (1980) derived Figure 1.

Before the flare of Moore and LaBonte, there was a large chromospheric filament suspended in the core field as sketched in Figure 1; the bottom of this filament was well above normal chromospheric heights. This filament (and the core field holding it) erupted during the birth of the chromospheric flare ribbons. In addition to this large high filament that erupted, there was another much lower filament that traced the polarity dividing line under the large filament. This lower filament did not erupt, but remained in place throughout the flare. The flare ribbons began against each side of the low filament and spread away from it as the flare progressed. These observations indicate that there was a lower part of the core field that did not erupt. Many flare filament eruptions show this bifurcation in which a lower filament or lower part of the filament stays put while the upper part erupts (Tang, 1986). Only the erupting part of the core field is sketched in Figure 1. In this model 3-D configuration, under the preflare envelope arcade the stationary lower part of the core field would be rooted closer to the polarity dividing line than is the upper part that reconnects and erupts. The downward product of this reconnection, the earliest and innermost loops of the flare arcade, would then straddle the underlying unreconnected remainder of the core field. One of these first inner loops of the flare arcade is shown in the sketch on the right side of Figure 1. It is also plausible that the lower, unerupted part of the core field in the Moore and LaBonte flare was similar to the upper part in having elbows that looped to low coronal heights. If so, these elbows remained after the flare eruption and were present in the late phase. Thus, late-phase core-field coronal elbows, such as in Figure 5, fit naturally into the 3-D field configuration of Figure 1. This further supports the view that the observed late-phase core-field elbow presented in this paper is typical rather than exceptional for large two-ribbon flares.

In Figure 1, as in the field configuration observed in and before the onsets of many large two-ribbon eruptive flares, there are core-field coronal elbows on both ends of the envelope arcade. In the late phase of our flare, a coronal elbow was visible at only one end of the flare arcade. It could be that in our flare the preflare core field was less symmetric than in Figure 1; perhaps there was more magnetic flux in the northern elbow than in the southern elbow, so that the southern elbow was not as prominent as the northern elbow. In this case, if the eruption opened equal amounts of magnetic flux from both elbows (as in Figure 1), after the eruption there would be an even greater asymmetry in the remaining elbows, the southern elbow now being even less prominent relative to the northern elbow than before the eruption. Another equally plausible possibility is that a southern elbow comparable to the northern elbow was present late in our flare, but its coronal reaches were not

as well connected to the subflaring under the flare arcade, hence did not participate as flaring arches, and so were not visible in Hα.

In closing, the observations presented in this paper and the above considerations support the following conclusions: (1) there was an S-shaped sheared core field with a coronal elbow on at least one end late in the large two-ribbon flare of 25–26 June, 1992; (2) such coronal core-field elbows are probably a common feature of the 3-D magnetic field configuration late in large two-ribbon flares; (3) the presence of coronal core-field elbows in the late phase is entirely compatible with the preflare 3-D field configuration and eruption scenario sketched in Figure 1. Because of their compatibility with the preflare 3-D configuration of Figure 1, the late-phase observations presented in this paper give futher confirmation to this model. Hirayama (1974) was the first to propose a 3-D field model along the lines of Figure 1 for eruptive two-ribbon flares. In Hirayama's model, as in Figure 1, the flare begins when the core field holding the filament erupts, allowing the legs of the envelope field to collapse together under the ascending core flux rope and reconnect to form and heat the growing flare arcade and spreading flare ribbons. However, in contrast to the preflare field configuration in Figure 1, in Hirayama's model the preflare envelope field was open instead of closed, and the preflare 3-D configuration of the core field was left unspecified. The late-phase observations presented in this paper, the recent filament-holding 3-D field model of Antiochos, Dahlburg, and Klimchuk (1994), and the recent *Yohkoh* SXT images of the coronal magnetic configuration at and before the onsets of large, eruptive, long-duration, two-ribbon flares reinforce each other in supporting the modified Hirayama picture in Figure 1: the preflare envelope field is closed, and the preflare core field is S-shaped and has coronal elbows.

Acknowledgements

First and foremost, we are indebted to Dr D. M. Rabin for his original insight that spawned this paper. We are greatful to Drs H. Kurokawa and R. Kitai for providing the Hida Observatory high-resolution Hα image for Figure 2. We thank the *Yohkoh* SXT team for providing the SXT data for Figure 3, and we thank Dr D. A. Falconer for preparing Figure 3.

References

Antiochos, S. K, Dahlburg, R. B., and Klimchuk, J. A.: 1994, *Astrophys. J.* **420**, L41.
Dodson-Prince, H. W. and Bruzek, A.: 1977, in in A. Bruzek and C. J. Durrant (eds.), *Illustrated Glossary for Solar and Solar-Terrestrial Physics*, D. Reidel Publ. Co., Dordrecht, Holland, p. 81.
Fontenla, J. M., Švestka, Z., Fárník, F., and Tang, F. Y.: 1991, *Solar Phys.* **134**, 145.
Gary, G. A., Moore, R. L., Hagyard, M. J., and Haisch, B. M.: 1987, *Astrophys. J.* **314**, 782.
Hirayama, T.: 1974, *Solar Phys.* **34**, 323.
Hudson, H. S., Acton, L. W., and Freeland, S. L.: 1996, *Astrophys. J.* **470**, 629.

Malherbe, J. M., Tarbell, T., Wiik, J. E., Schmieder, B., Franck, Z., Shine, R., and van Driel-Gesztelyi, L.: 1997, *Astrophys. J.* **482**, in press.
Manoharan, P. K., van Driel-Gesztelyi, L., Pick, M., and Démoulin, P.: 1996, *Astrophys. J.* **468**, L73.
Martin, S. F. and Švestka, Z. F.: 1988, *Solar Phys.* **116**, 91.
Martin, S. F., Bilimoria, R., and Tracadas, P. W.: 1994, in R. J. Rutten and C. J. Schrijver (eds.), *Solar Surface Magnetism*, Springer-Verlag, Berlin, p. 303.
Moore, R. L., and LaBonte, B. J.: 1980, in M. Dryer and E. Tandberg-Hanssen (eds.), *Solar and Interplanetary Dynamics*, D. Reidel Publ. Co., Dordrecht, Holland, p. 207.
Moore, R. L. and Roumeliotis, G.: 1992, in Z. Švestka, B. V. Jackson, and M. E. Machado (eds.), *Eruptive Solar Flares*, Springer-Verlag, Berlin, p. 69.
Moore, R. L., LaRosa, T. N., and Orwig, L. E.: 1995, *Astrophys. J.* **438**, 985.
Moore, R., McKenzie, D. L., Švestka, Z., Widing, K. G. *et al.*: 1980, in P. A. Sturrock (ed.), *Solar Flares*, Colorado Associated University Press, Boulder, Colorado, p. 341.
Moore, R. L., Hudson, H. S., Lemen, J. R., Shibata, K., Hirayama, T., and Ogawara, Y.: 1996, oral and poster presentation at Workshop on Measurements and Analyses of the 3-D Solar Magnetic Fields, held in Huntsville, Alabama, 9–11 April 1996, in preparation for publication.
Pevtsov, A. A., Canfield, R. C., and Metcalf, T. R.: 1995, *Astrophys. J.* **440**, L109.
Pevtsov, A. A., Canfield, R. C., and Zirin, H.: 1996, *Astrophys. J.* **473**, 533.
Rust, D. M. and Kumar, A.: 1996, *Astrophys. J.* **464**, L199.
Schmieder, B., Démoulin, P., Aulanier, G., and Golub, L.: 1996a, *Astrophys. J.* **467**, 881.
Schmieder, B., Heinzel. P., van Driel-Gesztelyi, L., and Lemen, J. R.: 1996b, *Solar Phys.* **165**, 303.
Shibata, K.: 1996, in Y. Uchida, T. Kosugi, and H. S. Hudson (eds.), *Proc. IAU Colloq.* **153**, 13.
Švestka, Z., and Cliver, E. W.: 1992, in Z. Švestka, B. V. Jackson, and M. E. Machado (eds.), *Eruptive Solar Flares*, Springer-Verlag, Berlin, p. 1.
Švestka, Z. F., Fárník, F., Fontenla, J. M., and Martin, S. F.: 1989, *Solar Phys.* **123**, 317.
Tang, F.: 1986, *Solar Phys.* **105**, 399.
Tsuneta, S.: 1996, in Y. Uchida, T. Kosugi, and H. S. Hudson (eds.), *Proc. IAU Colloq.* **153**, 161.
Tsuneta, S., Hara, H., Shimizu, T., Acton, L. W., Strong, K. T., Hudson, H. S., and Ogawara, Y.: 1992, *Publ. Astron. Soc. Japan* **44**, L63.
van Driel, L., Wiik, J. E., Schmieder, B., Tarbell, T., Kitai, R., Funakoshi, Y., and Anwar, B.: 1997, *Solar Phys.*, in press.